DOI: 10.3969/j.issn.1673-3185.2017.02.008 **http:** // english.ship-research.com

Translated from: XU J Q, XIONG Y, WANG Z Z. Numerical research of hydrodynamic performance of hybrid CRP podded propulsor in steering conditions[J]. Chinese Journal of Ship Research, 2017, 12(2): 63-70, 99.

Numerical research of hydrodynamic performance of hybrid CRP podded propulsor in steering conditions

XU Jiaqi, XIONG Ying, WANG Zhanzhi

Department of Naval Architecture Engineering, Naval University of Engineering, Wuhan 430033, China

Abstract: In order to study the influence of steering conditions on hybrid CRP podded propulsor, the calculation of the NACA0012 open-water rudder's lift coefficient was carried out by applying the RANS method combined with the SST k-ω turbulence model, and the near wall mesh arrangement and near wall treatment method applied in numerical calculation were selected through comparisons between the experimental results and the calculation results. The hydrodynamic performance of a podded propulsor was predicted on the basis of the above research, and the calculation results coincide with the experimental results. The object of the research was a hybrid CRP podded propulsor, and its hydrodynamic performance in steering conditions was predicted by applying our numerical method. Conclusions were drawn on the relationship between hydrodynamic performance parameters and steering angle, i.e., larger magnitudes of the after propeller thrust, pod horizontal force and steering moment will be acquired at larger steering angles, and the fore propeller thrust is basically as invariant as the pod steering. The internal reasons were also analyzed. Research shows that the propeller has good maneuverability, and will have wide application prospect.

Key words: hybrid CRP podded propulsor; steering conditions; numerical calculation; near wall treatment

CLC number: U661.31

0 Introduction

The concept of hybrid CRP podded propulsor was first introduced by ABB Company, and this type of propulsor combines the advantages of contra-rotating propeller (CRP) and podded propulsor: CRP redistributes the load of propeller, which reduces the load of fore propeller, thus reducing the diameter of propeller and increasing the gap between tip of blade and the hull to achieve the purpose of noise reduction and vibration reduction of the hull; at the same time, full-rotating pod cabin plays the role of rudder in the downstream of CRP[1]. Experiments showed that the propulsion system can improve the propulsion efficiency by 15%[2]. The model test and analysis of a naval depot ship T-AKE 1 after the installation of hybrid CRP podded propulsor indicated that compared with single-shaft and single-propeller arrangement, it can reduce the output power of main engine by 7%[3]. The 27th ITTC proposed to call this type of propulsor Hybrid Contra-Rotating Shaft Pod (HCRSP), and put forward the guide rule for open-water test on this type of propulsor[4].

At present, Sheng et al.[5-9] carried out numerical simulation to study the influence of axial distance between fore propeller and after propeller of propulsor, speed ratio and other design parameters on its hydrodynamic performance. What's more, experiment and numerical simulation were conducted on open-water performance under direct navigation condition and the influence of unsteady calculation time step and turbulence model on numerical simulation precision of open-water performance of CRP was also investigated, which is the main component of the propulsor.

Received: 2016-06-08

Supported by: National Natural Science Foundation of China (51479207)

Author(s): XU Jiaqi, male, born in 1991, master candidate. Research interest: hydrodynamic performance of ship. E-mail: 1578741698@qq.com

XIONG Ying (Corresponding author), male, born in 1958, Ph.D., professor. Research interest: hydrodynamic performance of ship.

Hybrid CRP podded propulsor shows great advantages in energy conservation and noise reduction, and the effect of steering conditions on its performance remains to be studied. Towed pod and pod of hybrid CRP podded propulsor are located in the downstream of propeller, which is equivalent to exert propeller wake on open-water rudder. Therefore, based on the lift coefficient prediction of open-water rudder at first, the paper obtains relatively reasonable near wall mesh arrangement and treatment, which are applied in the hydrodynamic performance prediction of podded propulsor under steering conditions. And the hydrodynamic performance of hybrid CRP podded propulsor under steering conditions is predicted on the basis of above, which lays the foundation for the design and engineering application of hybrid CRP podded propulsor.

StarCCM + software is adopted in the numerical simulation, which is based on the finite volume method. This software can integrate with ICEM and Solidworks, including a number of turbulence models, SIMPLE and PISO pressure correction algorithms, as well as a variety of difference schemes such as central difference, first order upwind and second order upwind. The software has many kinds of mesh partition technologies and mesh refinement technologies, and has the ability to self-judge the mesh quality. The software also contains various interface mesh technologies such as sliding mesh and overset mesh, and the attached non-structural mesh partition technology can better discretize the external flow field of complex geometries. The treatment of pod steering under steering conditions is achieved by overset mesh, which has great advantage in dealing with the large-amplitude relative motion between multiple bodies[10].

1 Mathematical model

Control equation includes continuity equation and momentum equation (RANS equation):

$$\frac{\partial \overline{u_i}}{\partial x_i} = 0 \tag{1}$$

$$\frac{\partial \overline{u_i}}{\partial t} + \frac{\partial (\bar{u}_i \bar{u}_j)}{\partial x_j} = -\frac{\partial \bar{p}}{\partial x_i} + \frac{\partial}{\partial x_j}\left(\eta \frac{\partial \overline{u_i}}{\partial x_j} - \rho \overline{u_i' u_j'}\right) \tag{2}$$

where "-" refers to time-average quantity; and " ' " refers to fluctuating quantity; and u, p, ρ, η refer to velocity, static pressure, fluid density and fluid dynamic viscosity, respectively; and $-\rho \overline{u_i' u_j'}$ refers to Reynolds stress.

The turbulence model uses the SST $k-\omega$ two-equation model[11], which introduces a mixed function that effectively combines the Standard $k-\omega$ model for solving near wall flow and the Standard $k-\varepsilon$ model for solving far-field flow.

2 Near wall treatment

The near wall region of numerical computational domain contains turbulent boundary layer physically, and due to the viscous damping of molecule near the wall, the turbulent fluctuation is gradually weakened. General high Reynolds number (Re) turbulence model, such as the SST $k-\omega$ two-equation model, is applied to the region with fully developed turbulence which has a certain distance from the wall, so corresponding treatment must be done[12].

The turbulent boundary layer can be approximately regarded as the composite layer of inner layer and outer layer. The inner layer includes viscous sublayer, transition layer and layer of logarithm law, and the outer layer includes velocity deficiency ratio layer and viscous upper layer[13]. The flow of the near wall region can be divided into the flow of wall region (including viscous sublayer, transition layer and layer of logarithm law) and the flow of the core region of turbulence. Two dimensionless parameters u^+ and y^+ are introduced to describe the flow characteristics of near wall region, as shown in Fig. 1. Their definitions are as follows.

$$u^+ = \frac{u}{u_\tau} \tag{3}$$

$$y^+ = \frac{\Delta y \rho u_\tau}{\mu} = \frac{\Delta y}{\mu}\sqrt{\frac{\tau_w}{\rho}} \tag{4}$$

where u_τ refers to the friction velocity of the wall, and $u_\tau = (\tau_w/\rho)^{1/2}$; τ_w refers to the shear stress of the wall; Δy refers to the distance from the wall; and μ refers to the dynamic viscosity.

Fig. 1 indicates the distribution law of time-average velocity along the normal direction of the wall. According to the value of y^+, the following conclusions can be drawn:

1) $y^+ < 5$ corresponds to the viscous sublayer. The time-average velocity and dimensionless wall distance present linear relationship (or linear law) as shown in Eq. (5):

$$u^+ = y^+ \tag{5}$$

2) $60 < y^+ < 300$ corresponds to the layer of logarithm law. The time-average velocity and dimensionless wall distance present logarithmic relationship (or called logarithm law) as shown in Eq. (6):

$$u^+ = \frac{1}{\kappa}\ln y^+ + C \tag{6}$$

where κ refers to the Von·Karman constant, which is about 0.40–0.41; C is another constant, and for smooth wall, $C \approx 5.0$–5.2[11].

The time-average physical quantity (such as time-average velocity) distribution of turbulent boundary layer along the normal direction of the wall can be described by wall law.

There are two kinds of wall laws in the software StarCCM + for numerical solution, which are standard wall law and mixed wall law. Several wall laws are included in the near wall treatment, and the near wall treatment is divided into the following three kinds.

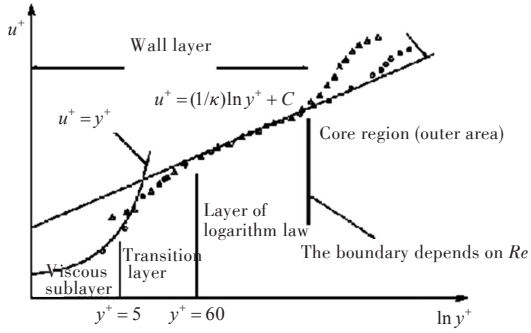

Fig.1 Near wall region division and time-average velocity profile

1) The idea of wall function method is adopted and standard wall law is applied in near wall treatment with high value of y^+. It is assumed that mesh nodes in the first layer of the near wall are in the layer of logarithm law of turbulent boundary layer. Among them, the wall function method contains a series of assumptions about the distribution of velocity, turbulence and other physical quantities in the near wall region. The method combining high Re turbulence model with wall function method dose not assign any nodes in the viscous sublayer, but arranges the first layer mesh nodes of the near wall in the region with fully developed turbulence[11].

2) Near wall treatment with low value of y^+ only applies to low Re turbulence model, and the method generally includes the solution to viscous sublayer, which requires finer near wall meshes.

3) Near wall treatment with full y^+ value is a mixed treatment method and should use mixed wall law.

3 Prediction of lift coefficient of open-water rudder

3.1 Calculating object

The aspect ratio of open-water rudder is 1.667, and its section aerofoil is NACA0012 and chord length c = 0.12 m. To reduce the workload of mesh generation under multiple attack angles, the interior domain contains open-water rudder and generates overset mesh with exterior domain. Prismatic layer mesh is arranged in the adjacent wall, and other part of interior domain uses non-structural tetrahedron mesh, while exterior domain uses hexahedron mesh. The distance from the boundary of interior domain to the upper and lower surfaces of open-water rudder is $7c$, and the distance to rudder blade end is 1.5c. The total computational domain is $30c \times 25c \times 10c$.

Three arrangement modes of near wall meshes are designed:

1) Scheme 1: the thickness of the first layer meshes is 1.68×10^{-5} m;

2) Scheme 2: the thickness of the first layer meshes is 6.0×10^{-4} m;

3) Scheme 3: the thickness of the first layer meshes is 1.2×10^{-3} m.

The layers for the prismatic layer meshes of scheme 1, scheme 2 and scheme 3 are 25, 7, and 7, respectively. The thickness growth rate of prismatic layer mesh is 1.05. The section of volume mesh is shown in Fig. 2.

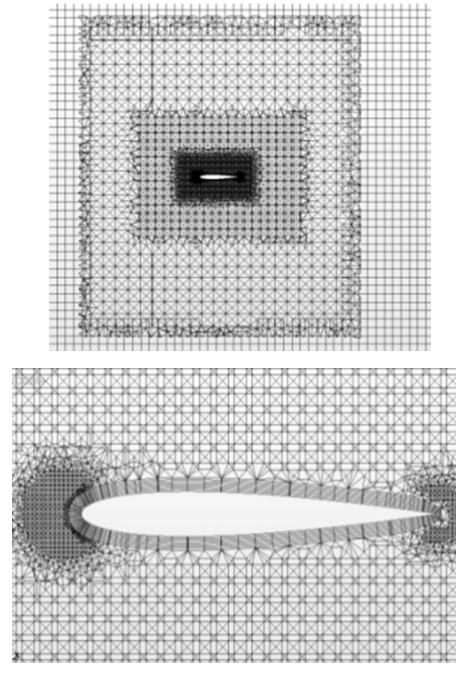

Fig.2 Open-water rudder mesh section

3.2 Numerical calculation method and boundary condition setting

Based on steady method, convection phase is discretized by second order format and SIMPLE algorithm is used to solve pressure-velocity coupling. With the use of SST $k-\omega$ turbulence model, scheme

1 adopts near wall treatment with full y^+ value and the other schemes adopt wall treatment with high value of y^+. The inlet is velocity inlet and the outlet is pressure outlet. The surface of open-water rudder and the upper and lower boundaries of exterior domain are no-slip impenetrable smooth walls. The inlet velocity V_A = 1.4 m/s, the outlet pressure p = 101 325 Pa, the density of water ρ = 997.513 kg/m^3, the dynamic viscosity $\mu = 9.017 \times 10^{-4}$ Pa·s, and the corresponding Re is 1.81×10^5 (in Reference [14], when Re is greater than 1.2×10^5, the test results are believed to be stable)

3.3 Influence of different near wall mesh schemes on the calculation results

The mean y^+ of the first layer meshes in the near wall obtained by 3 schemes is shown in Table 1, and the comparison between the calculation results and experimental results of lift coefficient of the open-water rudder[14] is shown in Fig. 3.

Table 1 First layer mesh thickness & mean y^+ value of different mesh plans

	Scheme 1	Scheme 2	Scheme 3
Mesh thickness of the first layer/mm	0.016 8	0.6	1.2
Mean y^+ value	0.95	34.58	83.67

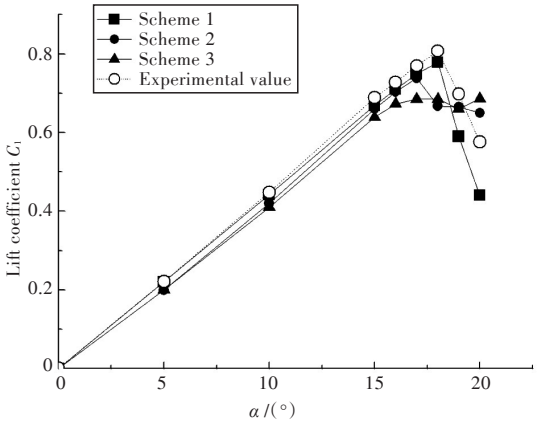

Fig.3 Comparison between calculation results & experimental results of open water rudder in different mesh plans

It can be seen from Fig. 3 that:

1) The calculation results of scheme 1 are closer to the experimental values than those of the rest schemes, and when $\alpha \leqslant 18°$, the error is less than 5%. The reason is that the laminar sublayer can be solved, which is more accurate than the wall function method without solving the laminar sublayer.

2) The calculation results of scheme 2 are closer to experimental values than those of scheme 3. The mean y^+ corresponding to scheme 2 is greater than 30, indicating that most of the mesh nodes of the first layer are located in the layer of logarithm law, which meets the basic requirements of the wall function method. However, the first layer meshes of scheme 3 are too thick, which makes the value of y^+ too large, so the simulation effect of the wall function method will be distorted when flow separation appears due to large rudder angle of open-water rudder.

The calculation results of lift coefficients under various attack angles are compared and evaluated comprehensively. Similar to scheme 1, the calculation results of lift coefficient of open-water rudder obtained by near wall mesh arrangement with $y^+ < 1$ and near wall treatment with full y^+ value are more reasonable.

4 Prediction of hydrodynamic performance of podded propulsor under steering conditions

4.1 Definition of hydrodynamic performance parameters

The hydrodynamic performance parameters of podded propulsor and the coordinate system are shown in Fig. 4, and the thrust and torque of propeller are always in the direction of propeller shaft. The positive direction of the steering angle δ is the clockwise direction when the pod is overlooked. At the moment, the pod deflects to the starboard. The positive direction of z-axis points to the lower part of propulsor (which is consistent with the coordinate direction in test[15]).

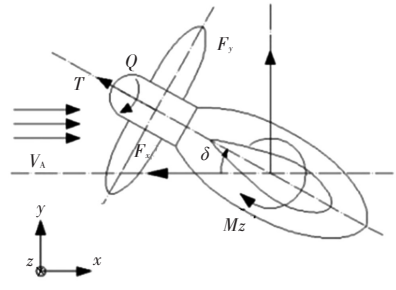

Fig.4 The hydrodynamic performance parameters, turning angle & coordinate system of podded propulsor

The advance coefficient, thrust and torque coefficient of propeller are defined as follows:

$$J = \frac{V_A}{nD}\ ;\ K_T = \frac{T}{\rho n^2 D^4}\ ;\ K_Q = \frac{Q}{\rho n^2 D^5} \qquad (7)$$

Axial force coefficient, horizontal force coefficient and vertical moment coefficient of pod unit are defined as:

$$K_{F_x}=\frac{F_X}{\rho n^2 D^4}\ ;\ K_{F_y}=\frac{F_Y}{\rho n^2 D^4}\ ;\ K_{M_z}=\frac{M_Z}{\rho n^2 D^5} \quad (8)$$

where F_x and F_y refer to axial force and horizontal force of pod unit; M_z refers to vertical moment of pod unit (steering moment); D refers to diameter of pod propeller; and n refers to rotational speed of pod propeller.

4.2 Geometric model and mesh partition

The podded propulsor is designed by Norwegian University of Science and Technology, and propeller model P-1374 used in test is designed by MARINTEK[15]. The main parameters of propeller model are shown in Table 2.

Table 2 Main parameters of propeller

Parameter	Value
Diameter of propeller D/mm	250
Diameter of hub d_h/mm	60
Designed pitch ratio	1.1
Roll angle/(°)	25
Expanded area ratio	0.6
Blade number and steering direction of propelle	Right steering and 4 blades

The length of pod is 181 mm and its maximum diameter is 92 mm. The height of strut is 300 mm, and the chord length and width of cross section are 86 mm and 42 mm respectively. Specific profiles of pod and strut are shown in Reference [15]. The surface mesh and volume mesh of podded propulsor are shown in Fig. 5.

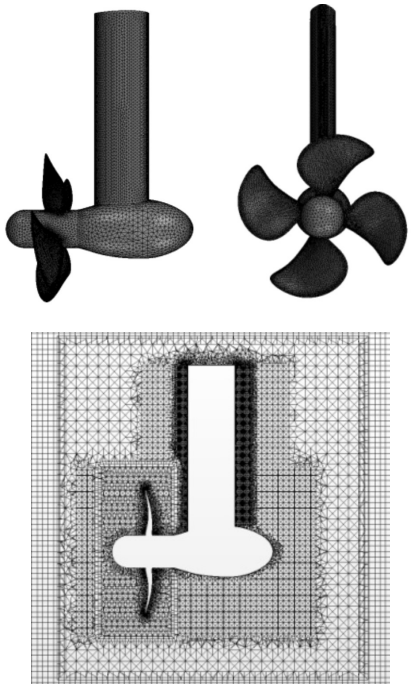

Fig.5 Podded propulsor mesh

25 layers of prismatic layer meshes are arranged close to the surface of the propeller blade and the hub, and the mesh thickness of the first layer is 0.006 mm. 25 layers of meshes are assigned on the surface of strut and pod, and the thickness of the first layer is 0.02 mm, with the thickness growth rate of prismatic layer mesh being 1.05. The computational domain is divided into three domains: pod steering domain, propeller rotation domain and far-field fixed domain. The propeller rotation domain and pod steering domain are fixed on the propeller and pod respectively, which are discretized into non-structural tetrahedron meshes. The propeller rotation domain and pod steering domain are connected by sliding mesh interface, and overset mesh is generated between pod steering domain and far-field fixed domain. The far-field fixed domain is discretized into hexahedral meshes. The total mesh number is about 5 million.

4.3 Numerical calculation method and boundary condition setting

The Moving Reference Frame (MRF) is firstly adopted to conduct steady-state computation so as to preliminarily calculate the flow field and save computation time. Then, sliding mesh method is used to perform unsteady calculation so that the unsteady flow characteristics and more accurate information of flow field can be captured. The propeller rotates 2.16° within one time step. The rotational speed of propeller is n = 6 s^{-1}, the advance coefficient is J = 0.6, the density of water is ρ = 999.04 kg/m^3, the dynamic viscosity is $\mu = 1.139\times10^{-3}$ Pa·s, and the inlet velocity V_A = 0.9 m/s. The settings of other boundary conditions are similar to those of the flow field of open-water rudder.

4.4 Comparative analysis of calculation result and experimental value

Numerical simulation and experiment are conducted under the towed conditions of podded propulsor, and the steering angle of podded propulsor is from -40° to 40°. With the interval of 10°, there are a total of 9 conditions. The analyzed hydrodynamic performance parameters include: thrust coefficient, torque coefficient, axial force coefficient, horizontal force coefficient and vertical moment (steering moment) coefficient of pod unit. The experimental value and calculation value are time-average values and the comparisons of calculation value and experimental value of each hydrodynamic coefficient are shown in Fig. 6. The relative error is shown in Table 3.

It can be seen from Fig. 6 that the variation trend of numerical calculation results and experimental results under different steering angles are in good agreement. The absolute values of horizontal force and steering moment of pod unit increase with the increase of steering angle.

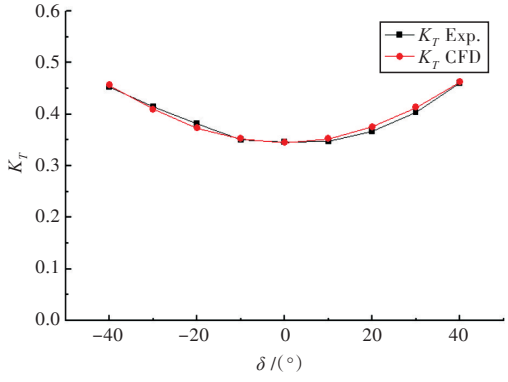

(a) Thrust coefficients

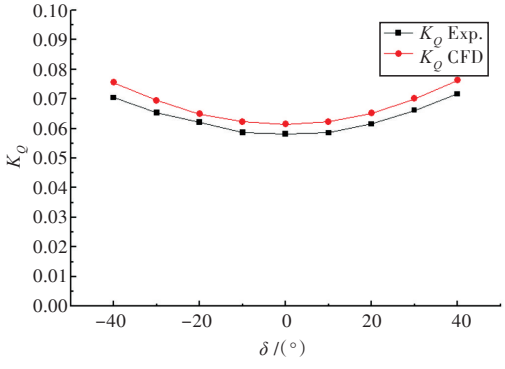

(b) Torque coefficients

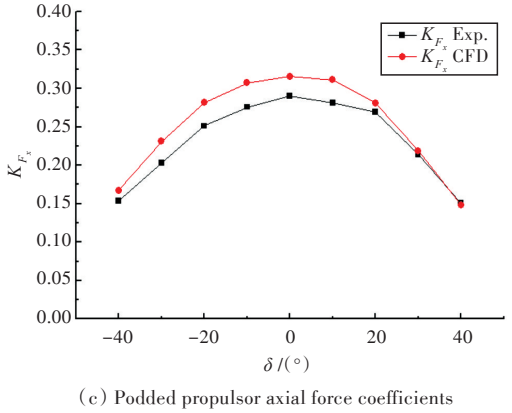

(c) Podded propulsor axial force coefficients

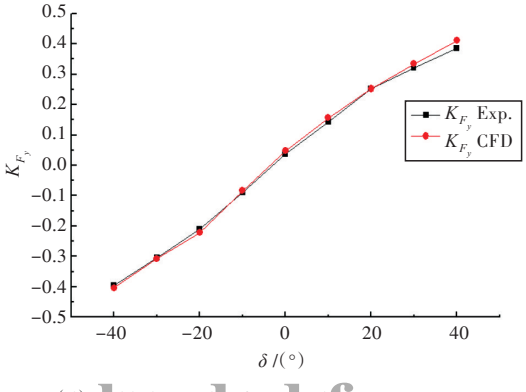

(d) Podded propulsor horizontal force coefficients

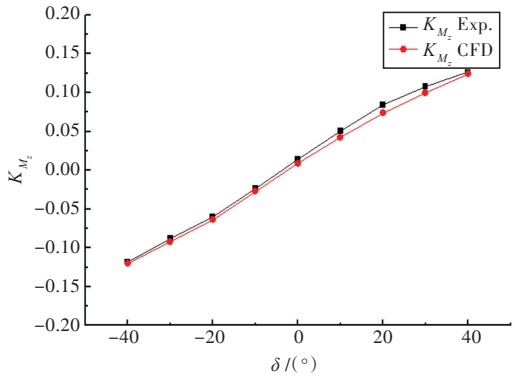

(e) Podded propulsor vertical moment(steering moment)coefficients

Fig.6 Comparison of podded propulsor hydrodynamic performance

Table 3 Relative error between calculation results & experimental results

δ /(°)	Relative error/%				
	K_T	K_Q	K_{F_x}	K_{F_y}	K_{F_z}
40	0.34	6.36	−1.32	6.42	−1.88
30	2.30	5.91	2.21	3.73	−7.55
20	2.11	5.95	4.40	0.11	−12.94
10	1.42	6.47	10.63	8.67	−15.39
0	−0.35	5.55	8.87	32.27	−38.56
−10	0.46	6.01	11.41	−7.61	14.91
−20	−2.12	4.34	12.04	5.66	5.72
−30	−1.02	6.34	14.04	0.85	4.97
−40	0.83	7.20	9.01	2.32	1.76

It can be observed from Table 3 that:

1) The relative error of thrust coefficient of propeller is within 3% and the relative error of torque coefficient is mostly less than 7%;

2) The relative error of axial force coefficient of pod unit is mostly within 10% and the error is relatively large when the pod turns to port, but still within 15%;

3) The relative error of horizontal force coefficient of pod unit is mostly within 7%, and when the steering angle is small, due to the small absolute value of coefficient, the relative error is large;

4) The relative error of vertical moment coefficient of pod unit is mostly within 13%, and due to the small absolute value of coefficient, the relative error is large when the steering angle is small.

5 Hydrodynamic performance prediction of hybrid CRP podded propulsor under steering conditions

5.1 Definition of hydrodynamic performance parameters

The hydrodynamic performance parameters and

coordinate systems are shown in Fig. 7 and both after propeller thrust and torque are in the propeller shaft direction. Seeing the ship bow from the stern, when the pod unit turns to left, the steering angle is positive, otherwise negative. The positive direction of z–axis points to the upper part of propulsor.

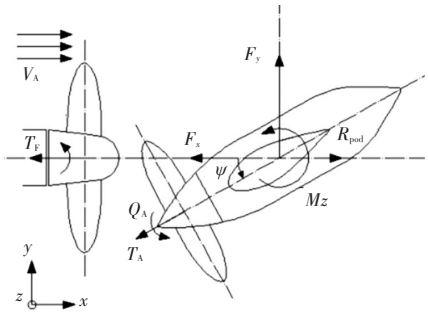

Fig.7 The hydrodynamic performance parameters, turning angle & coordinate system of hybrid CRP podded propulsor

The advance coefficient is defined by fore propeller parameter, and the rotational speed and propeller diameter in Eq. (7) are replaced with rotational speed of fore propeller n_F and diameter of fore propeller D_F.

Thrust coefficient of fore propeller K_{TF}, thrust coefficient of after propeller K_{TA}, torque coefficient of fore propeller K_{QF}, torque coefficient of after propeller K_{QA}, thrust coefficient of hybrid CRP podded propulsor K_T, torque coefficient K_Q and open-water efficiency η_0 are defined as follows:

$$K_{TF}=\frac{T_F}{\rho n_F^2 D_F^4};\quad K_{TA}=\frac{T_A}{\rho n_A^2 D_A^4};$$
$$K_T=\frac{T_F+F_x}{\rho n_F^2 D_F^4} \tag{9}$$

$$K_{QF}=\frac{Q_F}{\rho n_F^2 D_F^5};\quad K_{QA}=\frac{Q_A}{\rho n_A^2 D_A^5};$$
$$K_Q=\frac{n_F Q_F+n_A Q_A}{\rho n_F^3 D_F^5} \tag{10}$$

$$\eta_0=\frac{(T_F+F_x)V_A}{2\pi(n_F Q_F+n_A Q_A)} \tag{11}$$

where ρ refers to fluid density; n_A refers to the rotational speed of after propeller; D_A refers to the diameter of after propeller; T_F and T_A refer to the thrust of fore propeller and after propeller, respectively; Q_F and Q_A refer to the torque of fore propeller and after propeller, respectively; F_x is the component of pod unit force in the x–axis direction and is defined as follows:

$$F_x=T_A\cos\psi+R_{pod} \tag{12}$$

where R_{pod} refers to the resistance of pod cabin.

Three hydrodynamic performance coefficients are introduced under steering conditions:

$$K_{F_x}=\frac{F_x}{\rho n_A^2 D_A^4};\quad K_{F_y}=\frac{F_y}{\rho n_A^2 D_A^4} \tag{13}$$

$$K_{M_z}=\frac{M_z}{\rho n_A^2 D_A^5} \tag{14}$$

where F_y refers to the component of pod unit force in the y direction.

5.2 Geometric model and mesh partition

The calculating object is hybrid CRP podded propulsor of a 4000TEU container ship designed by Naval University of Engineering, and the scaled ratio of the model is 1∶27.5. The distance between the centers of disk surfaces of fore and after propellers is 0.454 5 D_F, and the main parameters of fore propeller and after propeller are shown in Table 4. The detailed data of this kind of propulsor can refer to Reference [16].

Table 4 Main parameters of fore & after propeller

Parameter	Fore propeller	After propeller
Diameter/mm	240	203.636
Number of blades	4	5
Pitch ratio$(P/D)_{0.7R}$	1.162 2	1.302 7
Hub diameter ratio	0.227	0.216
Section type	NACA66 mod/a=0.8	NACA66 mod/a=0.8
Steering direction	Left steering	Right steering

The length of pod is 278.65 mm and its maximum diameter is 90.9 mm. The height of the strut is 209.1 mm and the chord length of cross section is 145.46 mm, with the maximum thickness of the section being 45.35 mm. The side view of the hybrid CRP podded propulsor is shown in Fig. 8 and the mesh partition is shown in Fig. 9.

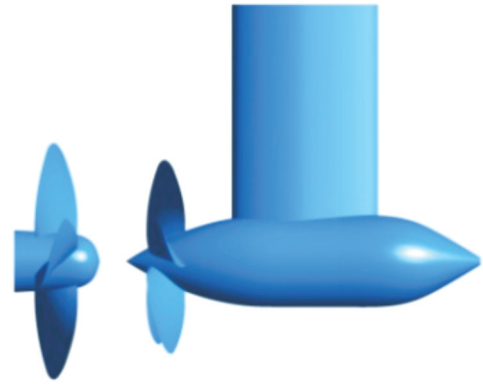

Fig.8 Hybrid CRP podded propulsor side view

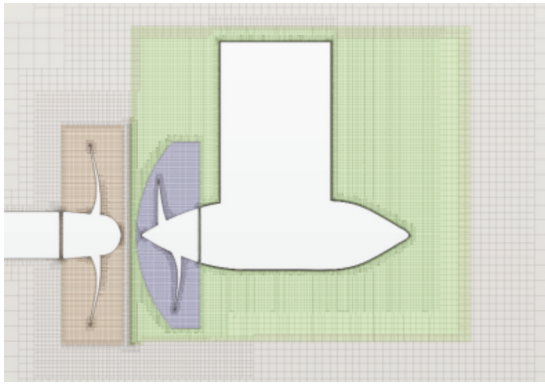

Fig.9 Mesh partition

The distance between velocity inlet of computational domain and disk surface of after propeller is $6.25D_F$, and the distances of pressure outlet and surrounding wall from the disk surface of after propeller are $15D_F$ and $7.5D_F$, respectively. The computational domain is divided into far-field fixed domain, fore propeller rotation domain, after propeller rotation domain and pod steering domain. The outer boundaries of fore propeller rotation domain and pod steering domain are set as overset mesh interface so that overset meshes are generated in far-field fixed domain, respectively. The after propeller rotation domain and pod steering domain are connected by the sliding mesh interface. The thicknesses of the first prismatic layer meshes of near wall of fore propeller and after propeller are set to be 0.24 mm and 0.2 mm respectively to ensure that y^+ value of blade surface is about 60, the prismatic layer meshes have 4 layers and the thickness growth rate between layers is 1.05. The thickness of the first prismatic layer meshes of pod near wall is 0.01 mm, and the y^+ value of pod surface is about 1. The prismatic layer meshes have 25 layers and the total thickness is 2.5 mm, with a thickness growth rate of 1.16. The total number of meshes is less than 6 million.

The speed of fore propeller n_F = 1 200 r/min and the speed ratio of fore propeller to after propeller n_A/n_F = 1.104. The other boundary condition setting and computing methods are similar to those of the podded propulsor and the time step corresponding to fore propeller rotation of 1.8° is adopted for unsteady calculation.

5.3 Hydrodynamic performance under steering conditions

Under the design condition of J = 0.781, the relationship of the time-average values of thrust coefficient, torque coefficient and open-water efficiency of hybrid CRP podded propulsor with steering angle ψ is shown in Fig. 10.

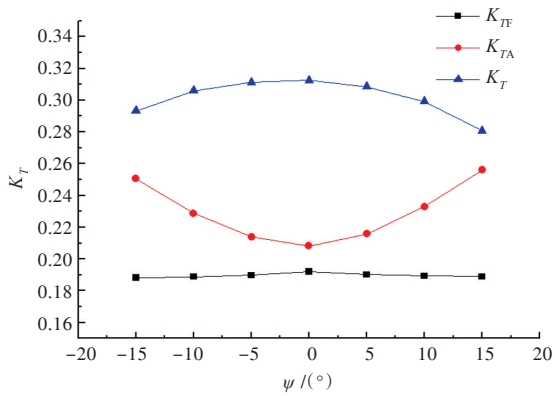

(a) Thrust coefficients

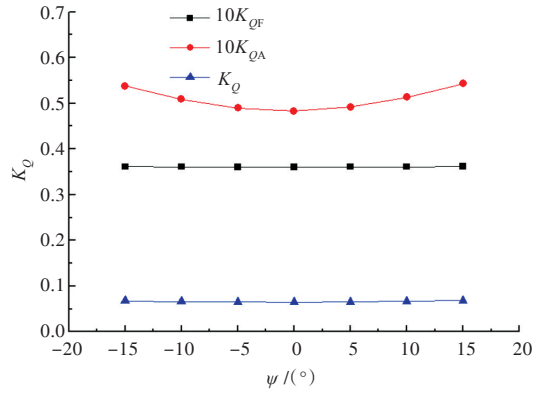

(b) Torque coefficients

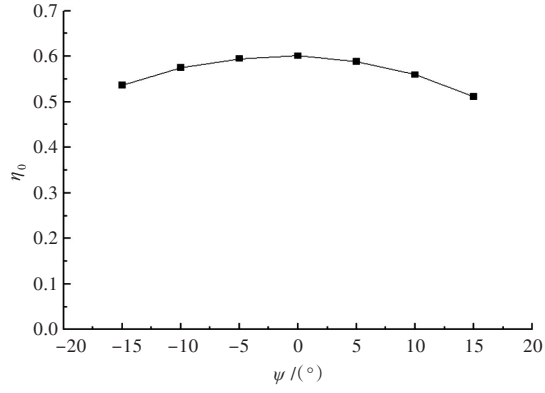

(c) Hybrid CRP podded propulsor open-water efficiency

Fig.10 Hybrid CRP podded propulsor hydrodynamic performance parameters

It can be seen from Fig. 10 that:

1) Thrust coefficient: with the increase of steering angle, the influence of wake acceleration driven by fore propeller on after propeller is weakened, the attack angle of after propeller blade section is increased and the increase amplitude of thrust coefficient of after propeller is large; and the thrust coefficient of fore propeller decreases slightly, whose decrease amplitude is less than 2%; the thrust coefficient of hybrid CRP podded propulsor decreases.

2) Torque coefficient: with the increase of steering angle, the attack angle of after propeller blade sec-

tion increases, the torque coefficient of after propeller increases, and the torque coefficient of fore propeller is almost unchanged; the torque coefficient of hybrid CRP podded propulsor also increases but its increase amplitude is smaller than that of the after propeller.

3) With the increase of steering angle, the open-water efficiency of hybrid CRP podded propulsor decreases.

The relationship of axial force coefficient K_{F_x}, horizontal force coefficient K_{F_y}, vertical moment coefficient (steering moment) of pod unit K_{M_z} with steering angle ψ is shown in Fig. 11.

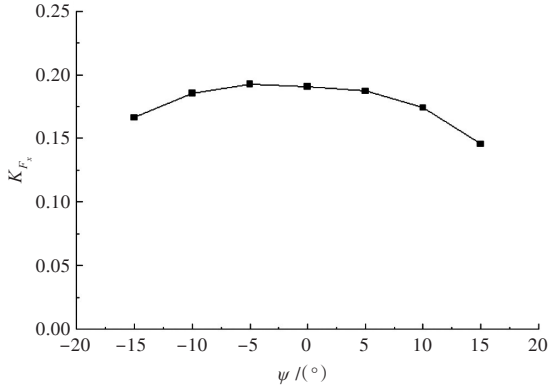

(a) Pod unit axial force coefficients

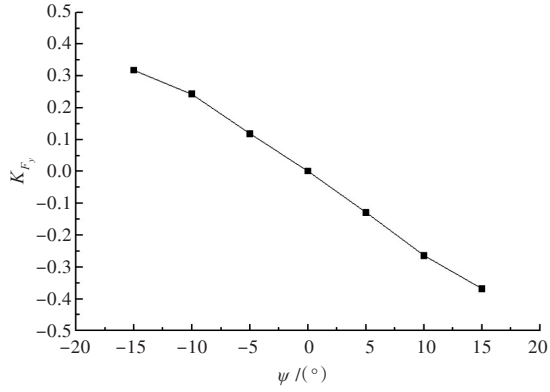

(b) Pod unit horizontal force coefficients

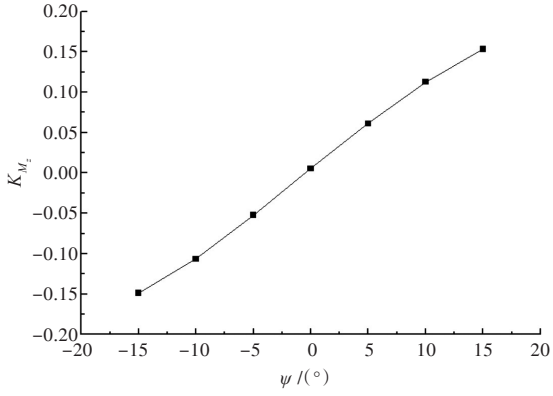

(c) Pod unit vertical moment coefficients

Fig.11 Hybrid CRP podded propulsor hydrodynamic performance parameters

It can be concluded from Fig. 11 that:

1) Axial force coefficient of pod unit K_{F_x} decreases with the increase of steering angle.

2) The absolute values of horizontal force coefficient of pod unit K_{F_y} and vertical moment coefficient (steering moment coefficient) of pod unit K_{M_z} increase with the increase of the absolute value of steering angle. When the pod turns to the port, the horizontal force applied on it points to the port and the vertical moment applied on it is along the positive direction of z-axis.

3) When the steering angle is zero, namely, direct navigation, the horizontal force coefficient of pod unit K_{F_y} and vertical moment (steering moment) coefficient of pod unit K_{M_z} are small positive values, especially the horizontal force on pod unit, which is almost zero and is much smaller than the horizontal force of towed poded propulsor under direct navigation. This may be because the rotating wake of the CRP arranged in front of the pod is weaker than that of single propeller.

6 Conclusions

Compared with high y^+ near wall treatment with thick first layer mesh, the first layer mesh of open-water rudder near wall ensures y^+ value less than 1, meanwhile, its combination of near wall treatment with full y^+ value can obtain more accurate lift coefficient calculation result. Similar near wall mesh and near wall treatment with full y^+ value can accurately predict the hydrodynamic performance of podded propulsor under steering condition. The hydrodynamic performance of a hybrid CRP podded propulsor is predicted and it is found that:

1) Fore propeller thrust does not change with steering angle and after propeller thrust increases with the increase of steering angle. The thrust of propulsor decreases with the increase of steering angle.

2) Axial force of pod unit decreases with the increase of steering angle and the horizontal force and vertical moment of pod unit increase with the increase of steering angle.

3) When the starboard and port turn, the horizontal force of the pod and the steering moment have the same value but opposite directions. When there is no turning, the horizontal force applied on the pod unit is small.

The above results show that this type of propeller has good maneuverability and will have wide applica-

tion prospect.

References

[1] UEDA N, OSHIMA A, UNSEKI T, et al. The first hybrid CRP-POD driven fast ROPAX ferry in the world [J]. Review Literature and Arts of the Americas, 2004, 41(6): 1-5.

[2] SÁNCHEZ-CAJA A, PÉREZ-SOBRINO M, QUEREDA M, et al. Combination of pod, CLT and CRP propulsion for improving ship efficiency: the TRIPOD project [C]//Third International Symposium on Marine Propulsors. Launceston, Tasmania, Austrilia: [s.n.], 2013.

[3] FORGACH K M, BROWN M J. Resistance and powering experiments with T-AKE model 5665-1 and hybrid contra-rotating shaft-pod propulsors phase 1 and phase 2: NSWCCD-50-T--2011/TBC [R]. 2011.

[4] 27th ITTC propulsion committee report presentation [C]//27th International towing tank conference. Copenhagen, Denmark, 2014.

[5] SHENG L, XIONG Y. Numerical simulation and experimental investigation on hydrodynamics performance of hybrid CRP podded propulsion [J]. Journal of Nanjing University of Aeronautics & Astronautics, 2012, 44 (2): 184-190 (in Chinese).

[6] WANG Z Z, XIONG Y. Effect of time step size and turbulence model on the open water hydrodynamic performance prediction of contra-rotating propellers [J]. China Ocean Engineering, 2013, 27(2): 193-204.

[7] WANG Z Z, XIONG Y, WANG R, et al. Numerical investigation of the scale effect of hydrodynamic performance of the hybrid CRP pod propulsion system [J]. Applied Ocean Research, 2016, 54: 26-38.

[8] WANG Z Z, XIONG Y, WANG R. Effect of the main design parameters on the open-water performance of a hybrid CRP podded propulsion system [J]. Journal of Harbin Engineering University, 2016, 37 (1): 98-103 (in Chinese).

[9] XIONG Y, ZHANG K, WANG Z Z, et al. Numerical and experimental studies on the effect of axial spacing on hydrodynamic performance of the hybrid CRP pod propulsion system [J]. China Ocean Engineering, 2016, 30(4): 627-636.

[10] WU Y Z, TIAN S L, XIA J. Unstructured grid methods for unsteady flow simulation [J]. Acta Aeronautica et Astronautica Sinica, 2011, 32(1): 15-26 (in Chinese).

[11] TAO W Q. 数值传热学 [M]. Xi'an: Xi'an Jiaotong University Press, 2001: 353-357(in Chinese).

[12] MENTER F R. Two-equation eddy-viscosity turbulence models for engineering applications [J]. AIAA Journal, 1994, 32(8): 1598-1605.

[13] CHEN M Z. Fundamentals of viscous fluid dynamics [M]. Beijing: Higher Education Press, 2002: 290-304 (in Chinese).

[14] LU H S, ZHU W W, FEI N Z, et al. Experimental study on open rudders [J]. Journal of Shanghai Jiao Tong University, 1981(2): 15-36(in Chinese).

[15] AMINI H. Azimuth propulsors in off-design conditions [D]. Trondheim: Norwegian University of Science and Technology, 2011.

[16] WANG Z Z. Study on the hydrodynamic characteristic and scale effect of a ship equipped with the hybrid CRP pod propulsion system [D]. Wuhan: Naval University of Engineering, 2014.

混合式CRP推进器操舵工况水动力性能数值研究

徐嘉启，熊鹰，王展智

海军工程大学 舰船工程系，湖北 武汉 430033

摘　要：[**目的**] 为了研究操舵工况对混合式CRP推进器水动力性能的影响，[**方法**] 采用RANS方法结合SST $k-\omega$湍流模型计算NACA0012型敞水舵的升力系数，通过与试验数据的对比，选定数值计算的近壁面网格布置和近壁面处理方式。在此基础上，进一步预报偏转工况下吊舱推进器的水动力性能，通过试验对比，表明误差在较小范围内。以混合式CRP推进器为研究对象，采用该数值方法预报操舵工况下该型推进器的水动力性能并予以分析。[**结果**] 研究发现，该型推进器后桨推力、吊舱横向力和操舵力矩均随偏转角的增大而增大，前桨推力基本不随偏转变化。[**结论**] 表明该型推进器操纵性能优良，具有广阔的工程应用前景。

关键词： 混合式CRP推进器；操舵工况；数值计算；近壁面处理方式